

CFD simulation of a venturi gas bubbles generator in a water-air system

Authors: ¹Ramiro Escudero G.*; ¹José E. Gembe H.; ²Martín Reyes P

ramiro1963@gmail.com; jose.g30@hotmail.com; mreyes@uaeh.edu.mx.

¹Institute of Research in Metallurgy and Materials. Universidad Michoacana de San Nicolás de Hidalgo. Santiago Tapia 403, C.P. 58000. Morelia, Michoacán, México.

² Academic Area of Earth and Materials Sciences, Universidad Autónoma del Estado de Hidalgo, México.

*Author to whom correspondence should be addressed

Abstract

The efficiency of the flotation process strongly depends on the characteristics of the gas dispersion: bubble diameter, gas holdup, and bubble surface area flux. Bubble size is important since it is responsible of colliding, attaching, and carrying the valuable species out of the column as concentrate; therefore, it is important to design spargers to control the gas dispersion characteristics and to increase the metallurgical performance of flotation. In this research work the Computational Fluid Dynamics (CFD) simulation method was applied to design and study the hydraulic phenomena that occur inside the sparger type venturi, when bubbles are generated. This sparger was simulated to be externally attached to a flotation column, and for a water-air system.

The CFD was solved through the software ANSYS Fluent R16.2®, and the preprocessor Gambit 2.4.6®. During the solution two turbulence models were assumed: k- ϵ , and LES; and the multiphase model: VOF.

The simulated venturi has the inlet and outlet diameter of 0.0381 m, whereas in the center the diameter is 0.0127 m (contracted vein). The convergent and divergent angles are of 15 degrees. Eight holes were radially distributed around the vein contract or throat of the venturi, to supply compressed air to the sparger.

Experimental results show that the bubble size and distribution of the bubbles swarm is more homogeneous when the gas is supplied through the eight orifices. The simulation results indicate that with the models VOF/k- ϵ both the dynamic pressure and phases velocity are not homogeneous inside the venturi, and when the bubbles swarm goes into the flotation column, a severe mixing is observed, caused by the appearance of zones with different density in the column. On the other hand, with the models VOF/LES the dynamic pressure and phases velocity are more uniform inside the sparger, ensuring an even bubble swarm distribution in the column.

Keywords: Fluid dynamic simulation, gas bubbles, ANSYS Fluent, venturi, VOF model

1. Introduction

During flotation, the size (d_b) and number of bubbles are directly related with the efficiency of this operation. Small bubbles increase the surface area of bubbles (S_b) available to transport valuable mass; nevertheless, very small bubbles, charged with hydrophobic particles, are not able to float and the bubble-solids aggregate are dragged by the tailings stream, decreasing the metallurgical performance of the column.

On the other hand, the type of bubble generator or sparger, is related to the continuity of the operation of the flotation device; the fail of the spargers installed inside the column, interrupts its operation being necessary to empty the column and change the dispersers blocked by limes from the pulp.

The phenomenon resulting from the swarm of bubbles with a wide size distribution is well known; the difference in diameters induces the appearance of zones with different density and when the system seeks to balance itself mechanically, an excessive mixing is produced, detaching from the bubbles the valuable species previously trapped by the gas dispersion [1].

The former facts lead to the need of designing bubble generators externally installed to the flotation column and that allow controlling de bubble diameter for a given application, even different from the concentration of minerals, maximizing the capacity of capture of hydrophobic species.

The mathematical design of gas spargers and the simulation of their operation in flotation systems is an attractive alternative that saves time and economic resources. The computational Fluid Dynamics (CFD) has become a useful simulation tool to understand the fundamental principles, physical, chemical, and hydrodynamic, taking place in unit operations that involve solids, liquids, and gas. The information obtained provides elements to design bubble generators, such as the venture-type sparger, its simulation during flotation processes allows to know different hydrodynamic behaviors during several operating conditions [2]

Trough CFD modeling, information is obtained on mechanisms and phenomena (recirculation, dispersion of phases, velocity and pressure profiles, etc.) which cannot be detected or observed during experimentation in the laboratory or during the operation at industrial plants [3].

In the present work, Computational Fluid Dynamics (CFD) simulation is used to design a venture-type disperser, to study the hydraulic phenomena that occur when generating the dispersion of bubbles inside it, for water-air system, making use of the ANSYS Fluent R16.2® and the Gambit 2.4.6® processor.

2. Equations of government

A typical three-dimensional fluid flow model solves the continuity equation and Navier-Stokes equations for incompressible Newtonian fluids which are based on the conservation of mass (one equation) and momentum (three equations) at each point on the computational domain. The solution of these equations provides the components of pressure and velocity in each of the points of the domain. At the high flow rates involved in this process, these models must incorporate turbulent fluid flows.

To fully describe the flow of a fluid, it is necessary to know the following properties of the system: density (ρ), pressure (P), velocity (V) in the three spatial directions of the system (u, v, w) corresponding to the axes (x, y, z). Since de system is made up of 6 unknowns, six equations are needed to find the solution to the three-dimensional flow. Along with the law of Ideal Gases, the five remaining equations are the Navier-Stokes ones [4, 5].

The Navier-Stokes equations (formulated by Claude-Louis Navier in 1822 and derived independently by George Gabriel Stokes in 1845) constitute a correct modeling of the Newtonian fluid flow, and they consist of a group of non-linear partial differential equations derived from the mass and moment conservation equations. Unfortunately they are extremely difficult to solve in their complete form; the following equations have been obtained from the FLUENT user manual [6].

2.1 Continuity equation

The first of the governing equations of fluids motion expresses the law of conservation of mass in the flow with density $\rho(x, y, z, t)$ and velocity $v(x, y, z, t)$.

$$\frac{\partial(\rho u)}{\partial x} + \frac{\partial(\rho v)}{\partial y} + \frac{\partial(\rho w)}{\partial z} = - \frac{\partial \rho}{\partial t} \tag{1}$$

2.2 Conservation of motion

The second law of Newton indicates that the velocity of change of movement of a particle in a fluid is equal to the sum of the forces acting on this particle.

Table 1.- Terms that each of the conservation equations of moment implies in the three spatial directions x, y, z (equation 2).

Component	Inertial term	Forces of the body	Gradient of pressure	Term of viscosity	Term source
X	$\rho \left(\frac{\partial u}{\partial t} + u \frac{\partial u}{\partial x} + v \frac{\partial u}{\partial y} + w \frac{\partial u}{\partial z} \right)$	$= \rho g_x$	$- \frac{\partial P}{\partial x}$	$+ \mu \left(\frac{\partial^2 u}{\partial x^2} + \frac{\partial^2 u}{\partial y^2} + \frac{\partial^2 u}{\partial z^2} \right)$	$+ F_b$

Y	$\rho \left(\frac{\partial v}{\partial t} + u \frac{\partial v}{\partial x} + v \frac{\partial v}{\partial y} + w \frac{\partial v}{\partial z} \right) = \rho g_y - \frac{\partial P}{\partial y} + \mu \left(\frac{\partial^2 v}{\partial x^2} + \frac{\partial^2 v}{\partial y^2} + \frac{\partial^2 v}{\partial z^2} \right) + F_b$
Z	$\rho \left(\frac{\partial w}{\partial t} + u \frac{\partial w}{\partial x} + v \frac{\partial w}{\partial y} + w \frac{\partial w}{\partial z} \right) = \rho g_z - \frac{\partial P}{\partial z} + \mu \left(\frac{\partial^2 w}{\partial x^2} + \frac{\partial^2 w}{\partial y^2} + \frac{\partial^2 w}{\partial z^2} \right) + F_b$

2.3 Turbulent flow

Turbulence is defined as the state of movement of a fluid in which the different relevant variables (pressure, velocity, etc.) fluctuate in a disorderly manner. It is a non-stationary state from the macroscopic point of view in which the different variables adopt dependent variables of both position and time and these values vary randomly and disorderly.

The resulting equations are like the Navier-Stokes equations in the sense that they have a derivative with respect to time in addition to convective, diffusive, and source terms. Also, the dissipation term appears which requires another differential equation to describe its transport. Several ways to solve this problem has been proposed through different approaches such as:

1. Direct Numerical Simulation (DNS),
2. Large Eddy Simulation (LES), and
3. Reynolds Averaged Navier–Stokes (RANS), among which is the k-ε model and the Reynolds Stress Model (RSM).

2.3.1 Large Eddy Simulation (LES)

The LES model is based on a mathematical filtering of the conservation equations by convolving them with different filtering functions which may be of spatial or frequency dependence. Commonly two spatial functions are used, one of rectangular type and another Gaussian and a frequency type filter low pass. In this filtering, all the variables of the equations are represented as the sum of one background component (filtered) and another fluctuating one. This results in the appearance of new variables in the system of equations that requires the use of additional expressions to close the system. Precisely these closing expressions constitute the modeling of the turbulent components of smaller spatial scale [7].

2.3.2 Model for the Reynolds Averaged Navier-Stokes (RANS)

The RANS models are based on the average of the equations of the fluid, for which all the magnitudes are replaced by the sum of their average value and a fluctuating component. After averaging, additional terms are obtained that require the addition of other equations to close the system. Two main variants of averages are presented: that of Reynolds and that of Favre; the latter uses averaged magnitudes per unit of mass [8]. Currently there are different methods or solution models for the RANS aimed at calculating a viscosity coefficient, among which we have:

2.3.2.1 Model k-ε

The mathematical model proposed by Jones and Launder, known as k-ε, is a semi-empirical model based on the modeling of transport equations for turbulent kinetic energy (k) and its dissipation (ε). The equation for k is derived from the exact equation, while that of ε was obtained by physical reasoning and maintains little resemblance to its exact mathematical equivalent. The derivation k-ε assumes that the flow is totally turbulent and that the effects of molecular viscosity are negligible. In this way, this model only applies to fully developed turbulent flows [9].

The equations for the turbulent kinetic energy and its dissipation velocity are the following [6]:

$$\rho \frac{\partial k}{\partial t} + \rho \frac{\partial k u_i}{\partial x_i} = \frac{\partial}{\partial x_j} \left[\left(\mu + \frac{\mu_t}{\sigma_k} \right) \frac{\partial k}{\partial x_j} \right] + G_k + G_b - \rho \varepsilon - Y_M + S_k \quad (2)$$

$$\rho \frac{\partial \varepsilon}{\partial t} + \rho \frac{\partial \varepsilon u_i}{\partial x_i} = \frac{\partial}{\partial x_j} \left[\left(\mu + \frac{\mu_t}{\sigma_\varepsilon} \right) \frac{\partial \varepsilon}{\partial x_j} \right] + C_{1\varepsilon} \frac{\varepsilon}{k} (G_k + C_{3\varepsilon} G_b) - C_{2\varepsilon} \rho \frac{\varepsilon^2}{k} + S_\varepsilon \quad (3)$$

Being G_k the generation of the turbulent kinetic energy due to the average velocity gradients, G_b the generation of turbulent kinetic energy due to the flotation forces, Y_m is the contribution of fluctuating dilation in compressible turbulence respect to total dissipation, $C_{1\epsilon}$, $C_{2\epsilon}$, and $C_{3\epsilon}$ are constants, σ_k and σ_ϵ are the turbulent Prandtl numbers for k and ϵ respectively, whereas S_k and S_ϵ are the source terms.

The turbulent viscosity (μ_t) is calculated by combining k and ϵ as follows:

$$\mu_t = \rho C_\mu \frac{k^2}{\epsilon} \quad (4)$$

Where C_μ is a constant; $C_{1\epsilon}$, $C_{2\epsilon}$, $C_{3\epsilon}$, C_μ , σ_k and σ_ϵ are constants with values: $C_{1\epsilon} = 1.44$, $C_{2\epsilon} = 1.92$, $C_\mu = 0.09$, $\sigma_k = 1.0$ and $\sigma_\epsilon = 1.3$.

2.3.3 Multiphase flow

Also called Fluid Volume Model (VOF) is applied for the modeling of multiphase flows by tracking the interface between the different phases (liquid, solid and gas). For a multiphase system that contains very small particles, bubbles or droplets that closely follow the continuous phase, reasonable simulations result can be achieved. Systems in which the dispersed phase has a large effect on the continuous phase are more difficult to simulate with precision, and only the ordinary models are available for multiphase systems with a high charge of the dispersed phase. At the moment, the quality of simulations is limited not only by the speed or memory of the computer, but the lack of good models for the multiphase flow; however, multiphase flows are very important in engineering, since many processes observe this type of flow.

The VOF model is suitable for stratified flow, free surface flows and movement of large bubbles in liquids; although, it is not applicable for a system with many drops or very small bubbles [6, 9].

3. Materials and methods

Mathematical simulation techniques were applied to solve numerically the parameters of dynamic fluids of the venturi-type disperser, supported by the CFD through the software ANSYS Fluent 16.2.

To study the hydrodynamic behavior generated by the bubble formation inside the disperser, first a venturi with only one air intake was designed, located right in the center of the throat (Figure 1).

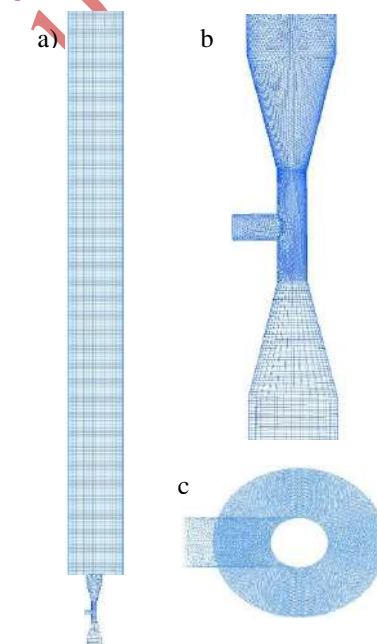


Figure 1. Design and meshing of the venturi-type disperser with only one air intake: a) venturi connected in the outer base of the column; b) design of the venturi; c) configuration of the air intake.

The design and meshing was made by using the software Gambit 2.4.6. The simulated column is 2.77 m in height and 0.10 m in diameter. The venturi is 0.21 m in length and it is constituted for three sections: the throat (0.0127 m diameter); the input and output zones with largest diameters of 0.0381 m. To avoid bubbles coalescence due to wall effects, the convergent and divergent angles are 15 degrees [10, 11, 12]. The meshing is composed by a structured one in the input of the venturi and in the flotation column, whereas in the throat and the divergent part of the disperser, a finest mesh (hybrid type) was used to obtain a better detail in the simulating results.

In a second part of simulation, a venturi with eight air intakes radially distributed was designed, to allow a better distribution of bubbles in the cross-sectional area of the venturi. To ensure an even air supply through every intake, individual rotameters were installed, one for each air intake. Each gas intake is 0.016 m in diameter. Figure 2 shows the modified venturi with the described meshing, the total number of nodes is 966, 310.

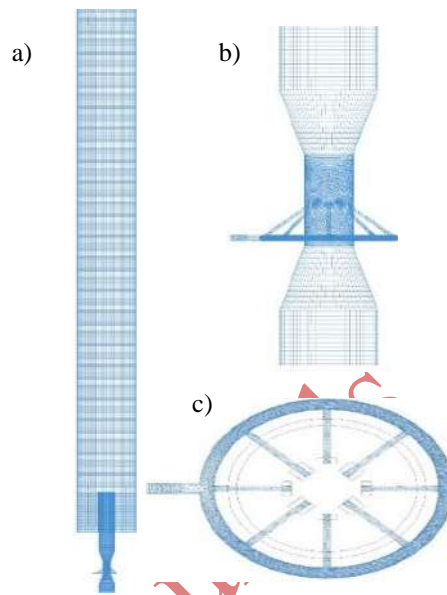


Figure 2. Design of meshing for the venturi with eight air intakes: a) venturi located in the outer base of the column; b) modified venturi-type disperser; c) distribution of the air intakes.

During simulations, the VOF multiphase and the $k-\varepsilon$ turbulence models were applied; in the last design, together with the $k-\varepsilon$, the LES model was used. The simulations were made for air-water system, and the initial conditions are shown in Table 1. The criterion of convergence of the residuals was taken 10^{-3} for each component in the residual scale. The chosen time step was 5×10^{-5} .

Table 1. Operating conditions used during the simulation.

Condition	
Liquid phase	
Density	1000 kg m ⁻³
Viscosity	0.001003 kg m ⁻¹ s ⁻¹
Superficial velocity	0.22 m s ⁻¹
Gas Phase	
Density	1.225 kg m ⁻³
Viscosity	1.7894 x 10 ⁻⁵ kg m ⁻¹ s ⁻¹
Superficial velocity	33.16 m s ⁻¹

4. Results and discussion

The results from simulation of a single air intake are shown in Figure 3. The first bubbles coalesce generating bigger bubbles; this is because at the beginning the air has the difficulty of breaking the forces of attraction between the water molecules, so it is easier to accumulate air in larger bubbles. It is expected that these bubbles will generate a strong mixing when entering in the column.

The velocity contours allow to observe another phenomenon that occur within the venturi, a recirculation in the discharge zone of the disperser, which is caused by the displacement of liquid by the bubbles; this flow of water increases with the bubble size (see Figure 3b). According to some authors, this effect results in coalescence of bubbles [13, 14].

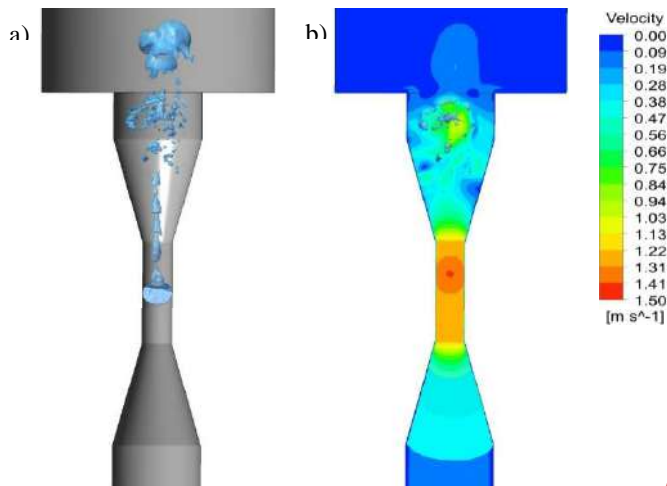


Figure 3. a) CFD image of the generation of bubbles with the first venturi type disperser, b) velocity contours generated inside the venturi.

With the purpose to generate a swarm of bubbles with a homogeneous size distribution and evenly distributed inside the disperser, the feed of air to the venturi through eight intakes radially located around the throat of it, was simulated. Despite showing some improvement in the distribution of the bubbles, can be observed in Figure 4 a tendency of bubbles to move close to the walls of the venturi, causing also coalescence; on the other hand, in Figure 4b) is observed the same trend but in terms of the contour velocity.

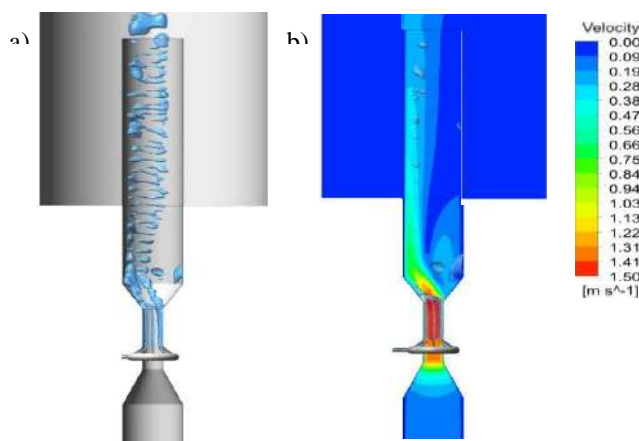


Figure 4. a) Imagen CFD de la generación de burbujas con el diseño de 8 entradas del dispersor tipo venturi; b) contornos de velocidad generados en el interior del dispersor.

Trying to avoid the last behavior of the bubbles, the air inlets were introduced 0.0012 m into the venturi, as shown in Figure 2.

With the last design of venturi a set of mathematical simulations were run by combining the multiphase model VOF with the turbulence models $k-\epsilon$ and LES.

It is widely known the relationship between the gas holdup, bubble size, and bubble surface area flux in the collection zone of the column; Figure 5 shows the results from simulating the bubbles generation with the venturi type disperser, through the models of turbulence: $k-\epsilon$ and LES.

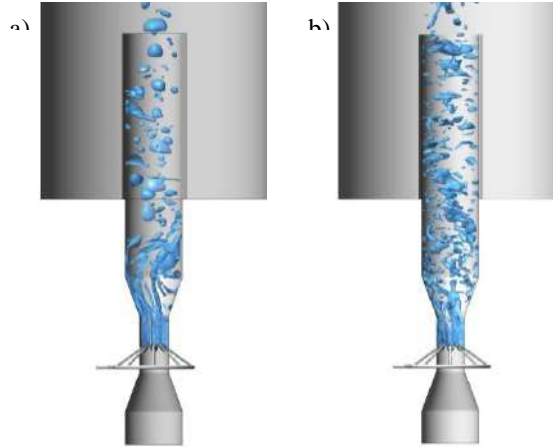


Figure 5. CFD image of the generation of bubbles with the venturi type disperser, a) simulation with $k-\epsilon$; b) simulation with LES.

A difference exists between the simulation models in terms of the dispersion and bubble size. The simulations made with the model $k-\epsilon$ have bubbles with larger size (Figure 5a); this is caused by phenomenon of coalescence, derived from the recirculation that occurs in the convergent area of the venturi; in addition, the great part of the flow of bubbles is channeled through certain zone of the column. This fact very probably will cause a certain grade of mixing.

From Figure 5b) it is possible to establish that the solution obtained from the model LES is closer to what occurs in practice, since the swarm of bubbles tends to cover most of the cross-sectional area of the discharge zone of the venturi. Another important point is the size of bubbles, which is smaller in this case, and its size distribution is more homogeneous.

Figure 6 shows the gas holdup distribution within the first 0.6 m of the column. The $k-\epsilon$ model predicts very low gas holdup values in certain zones of the column whereas in some other regions the fraction of gas is maximum; this fact infers the appearance of excessive mixing because the existence of zones with different density. The LES model for its part, presents a better distribution of the gas holdup in the column, which should avoid the excessive mixing in the flotation column.

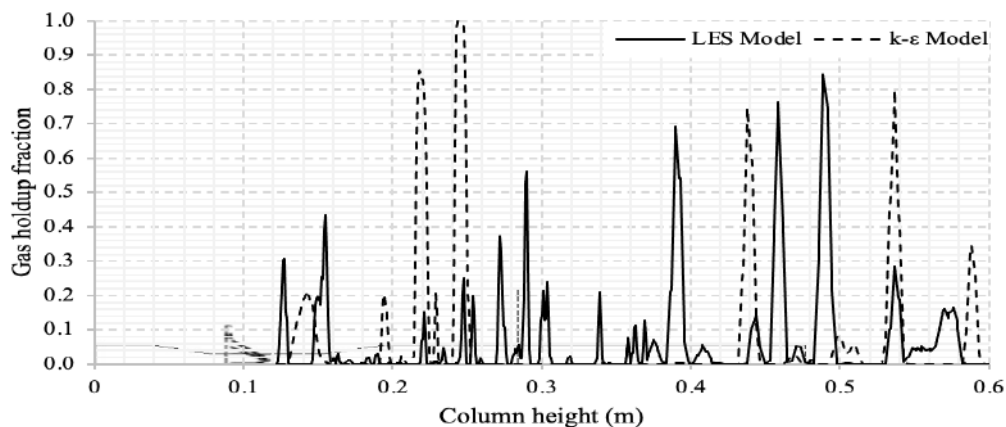


Figure 6. Distribution of the gas holdup along the venturi and within the first 0.6 m of the column. $k-\epsilon$, and LES models.

The velocity contours show the different profiles from the flows of liquid and the bubbles swam. Due to the venturi effect and complying with the continuity equation, a gradient velocity exists when a fluid flows through a narrower area. When air encounters the water flow, the bubbles form and tend to float because of the difference in density; as the bubbles move, they shift water, which causes variations in the velocities of the phases, as observed in Figure 7. The maximum velocity occurs in the contracted vein. The simulation made with the $k-\epsilon$ model presents an increase in the velocity towards the side where the recirculation is generated. On the other hand, in the simulation with the LES model, there is not tendency of the velocity, what is shown are the oscillations caused by the flotation of the bubbles, this due to the greater number of bubbles and a more homogeneous size [15]. The velocity profiles are shown schematically in Figure 8.

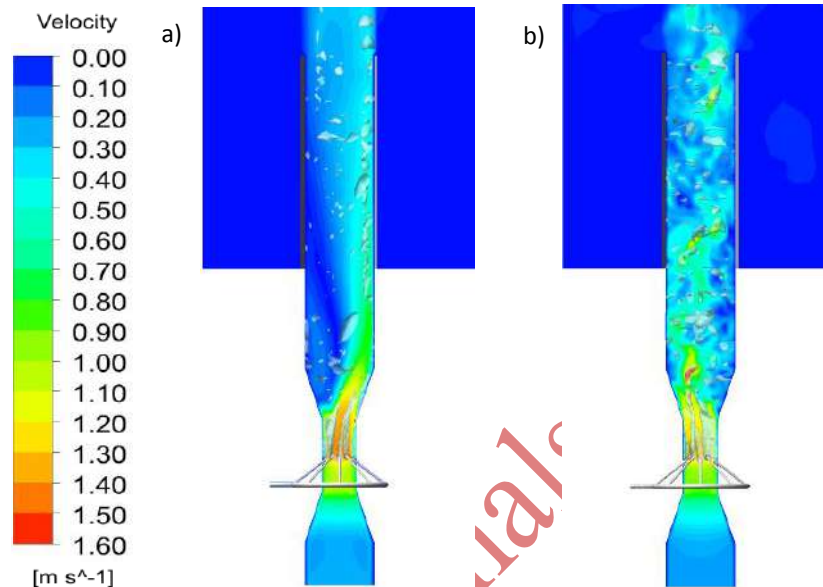


Figure 7. Velocity contours generated inside the venturi; a) simulation with the $k-\epsilon$ model; b) LES simulation model.

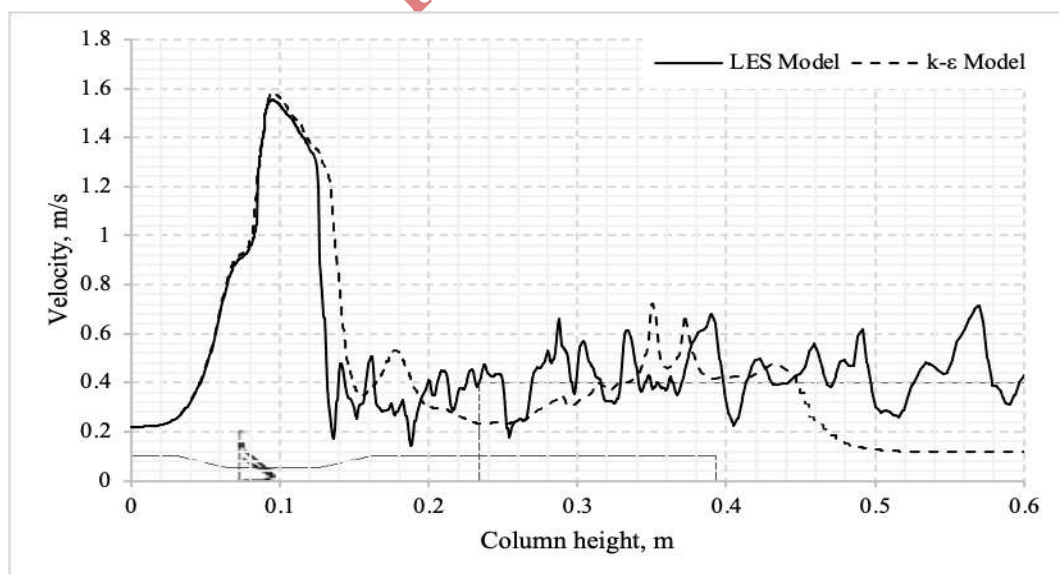


Figure 8. Velocity profiles along the venturi and in the first 0.6 m within the column. $k-\epsilon$, and LES models.

Regarding the increase in the pressure drop that is generated inside the venturi by the diameter reduction, from Figure 9 it can be observed this divergence is caused by the difference in diameters. As there is much greater dynamic pressure in the throat, the system seeks mechanical balance (pressure reduction), for this the system absorbs the air that is supplied in the central part of the throat, accumulating energy that is released in the form of bubbles when leaving the venturi.

In the simulation of the $k-\epsilon$ model the dynamic pressure is not homogeneous and is preferably increased on one side of the venturi; this due to the recirculation of phases in this area, which is in the same side where pressure is increased [16]. On the contrary, the simulation with the LES model presents a more uniform distribution of the dynamic pressure, transverse and longitudinally in the disperser, assuring the uniform distribution of bubbles in the column.

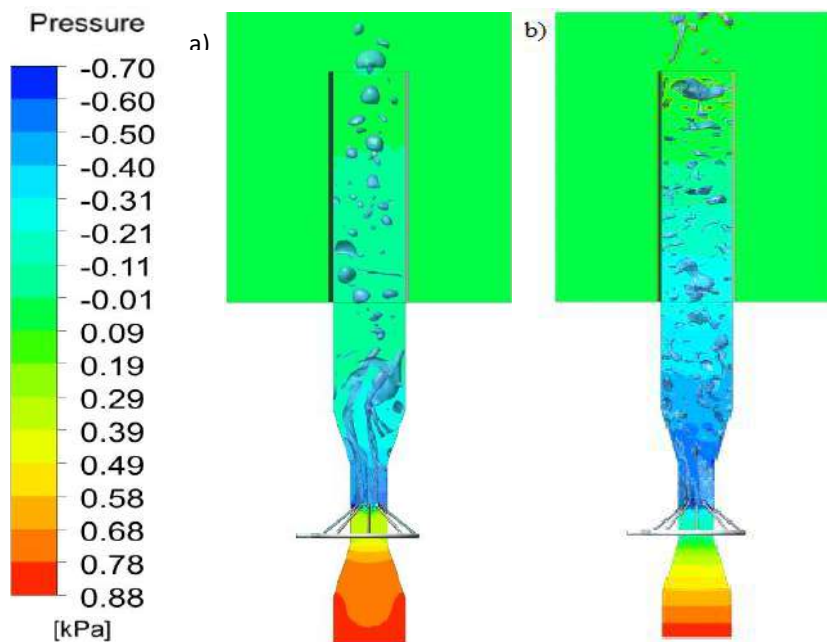


Figure 9. Dynamic pressure profiles generated within the venturi-type disperser; a) simulation with the $k-\epsilon$ model, b) LES model.

By means Figure 10, it is easy to observe the differences in dynamic pressure generated by the simulated disperser, through the two models. The LES model presents a more homogeneous distribution of the dynamic pressure; this behavior is very like the velocity, since the dynamic pressure is generated from the force with which the liquid is displaced and then the two phases: liquid and air.

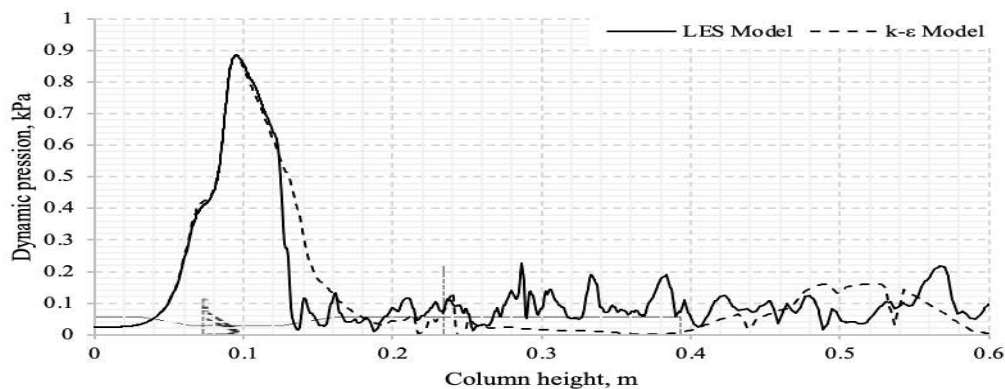


Figure 10. Dynamic pressure generated along the venturi and the first 0.6 m of the column. $k-\epsilon$, and LES models.

Conclusions

From the mathematical simulation to numerically solve the parameters of dynamic fluids, using the ANSYS Fluent software, which allows to design and predict the hydrodynamic behavior of the phases in the output of a venturi-type disperser, the following conclusions are drawn:

The modifications made to the venturi disperser allowed to improve the fluid dynamics generated inside the sparger; with the increase of the number of air inlets it was contributed to obtain a better distribution of the bubble swarm in the cross-sectional area of the disperser; whereas with the deeper introduction of the air intakes, the recirculation caused by the tendency of the bubbles towards the side of the venturi was reduced.

In the simulation using the VOF and k- ϵ models, the output variables: dynamic pressure and phase velocities, are not homogeneous inside the disperser. By entering the swarm of bubbles to the column creates zones of different density that causes recirculation and mixing.

The results of the simulation with the VOF-LES models indicate distributions of the dynamic pressure and fluid dynamics more uniform, transverse and longitudinally in the disperser, guaranteeing the uniform distribution of bubbles in the column.

References

- [1] Clayton R, Jameson GJ, Manlapig EV, The development and application of the Jameson cell. *Minerals Engineering*, 4(7): p. 925-933. 1991.
- [2] Madrid RG, Evaluación por modelación CFD del proceso de flotación en una celda de agitación mecánica y del efecto de la granulometría en la recuperación de mineral, in Facultad de Ciencias Físicas y Matemáticas. 2012, Universidad de Chile: Santiago, Chile.
- [3] Liu TY, Schwarz M, CFD-based modelling of bubble-particle collision efficiency with mobile bubble surface in a turbulent environment. *International Journal of Mineral Processing*, 90(1): p. 45-55. 2009.
- [4] Launder BE, Spalding DB, Lectures in mathematical models of turbulence. 1972.
- [5] Blazek J, Computational fluid dynamics: principles and applications. Butterworth-Heinemann. 2015.
- [6] FLUENT 14.5 *Theory Guide*. Chapter 6, 143-173. Canonsburg, PA, USA: ANSYS Inc, 2012.
- [7] Capote J, et al., Influencia del Modelo de Turbulencia y del Refinamiento de la Discretización Espacial en la Exactitud de las Simulaciones Computacionales de Incendios. *Revista internacional de métodos numéricos para cálculo y diseño en ingeniería*, 24(3): p. 227-245. 2008.
- [8] Wilcox D, Turbulence modeling for CFD. La Canada, California: DCW Industries. Inc, 5354: p. 124-128. 1998.
- [9] Launder BE, Spalding D, The numerical computation of turbulent flows. *Computer methods in applied mechanics and engineering*, 3(2): p. 269-289. 1974.
- [10] Ponasse M, et al., Bubble formation by water release in nozzle---II. Influence of various parameters on bubble size. *Water Research*, 32(8): p. 2498-2506. 1998.
- [11] Paladino, EE, Maliska CR, Computational modeling of bubbly flows in differential pressure flow meters. *Flow Measurement and Instrumentation*, 22(4): p. 309-318. 2011.
- [12] Sundararaj S, Selladurai V; Flow and Mixing Pattern of Transverse Turbulent Jet in Venturi-Jet Mixer. *Springer Science & Business Media B.V.*, 38(12), p. 3563-3573. 2013.
- [13] Grau RA, Laskowski JS, Role of frothers in bubble generation and coalescence in a mechanical flotation cell. *The Canadian Journal of Chemical Engineering*, 84(2), 170-182. 2006.
- [14] Diaz PP, Dobby G. Kinetic studies in flotation columns: bubble size effect. *Minerals Engineering*, 7(4), 465-478. 1994.
- [15] Olmo-Velázquez A, et al., Estudio y modelación del flujo bifásico líquido-gas para bajos valores de Reynolds. *Ingeniería Mecánica*, 18(1): p. 1-11. 2015.
- [16] Kim MI, et al., Numerical and experimental investigations of gas-liquid dispersion in an ejector. *Chemical Engineering Science*, 62(24): p. 7133-7139. 2007.